

Highlights

Reducing RES Droughts through the integration of wind and PV

Boris Morin, Aina Maimó Far, Damian Flynn, Conor Sweeney

- RES droughts are analysed using 45 years of hourly wind and PV generation data
- RES droughts from C3S-Energy and ERA5-Atlite datasets are compared
- Adding PV to a wind-dominated system reduces RES drought frequency and duration
- Validated RES datasets are crucial to accurately identify RES drought extremes

Reducing RES Droughts through the integration of wind and PV

Boris Morin^{a,*}, Aina Maimó Far^a, Damian Flynn^b, Conor Sweeney^a

*^aSchool of Mathematics and Statistics, University College Dublin, Belfield, Dublin
4, Dublin, D04 V1W8, Ireland*

*^bSchool of Electrical and Electronic Engineering, University College Dublin, Belfield,
Dublin 4, Dublin, D04 V1W8, Ireland*

*Corresponding author

Email addresses: `boris.morin@ucdconnect.ie` (Boris Morin),
`aina.maimofar@ucd.ie` (Aina Maimó Far), `damian.flynn@ucd.ie` (Damian Flynn),
`conor.sweeney@ucd.ie` (Conor Sweeney)

Abstract

Increasing the share of electricity produced from renewable energy sources (RES), combined with RES dependence on weather, poses a critical challenge for energy systems. This study investigates the importance of the balance between wind and photovoltaic (PV) capacity on periods of low renewable generation, known as RES droughts. Three different RES models are used to estimate the capacity factors for different scenarios of installed capacities for wind and PV power. The skill of the RES models is quantified by comparing capacity factor time series to observed hourly data and by assessing their representation of observed RES droughts. The RES models are used to generate a 45-year hourly time series of RES capacity factor, enabling analysis of the frequency, duration and return periods of RES droughts at a climatological scale. Results show the importance of using an accurate, validated RES model for RES drought risk assessment. The addition of PV capacity to a wind-dominated system results in a significant reduction in the frequency and duration of RES droughts, while also reducing extremes and seasonal drought patterns. These findings underscore the importance of diversification in RES capacity to enhance energy security and resilience.

Keywords: RES Drought, Wind Power, Solar PV Power, Renewable Energy Sources, Return Periods

1. Introduction

The EU aims to generate at least 69% of its electricity from renewable energy sources (RES) by 2030, up from 41% in 2022 [1]. While this transition is essential for reducing greenhouse gas emissions, it also highlights the challenge of managing the variability of weather-dependent energy sources such as wind and photovoltaic (PV) power. This challenge is compounded by the increasing electrification of energy sectors, which places greater demand on the power system and makes it more sensitive to meteorological conditions [2, 3, 4]. Periods of low renewable generation, known as *Dunkelflaute* or RES droughts, pose significant risks to system adequacy and energy security, emphasising the need for a resilient energy system to meet both growing electricity demand and decarbonisation targets.

This study focuses on Ireland, a region with a strong reliance on wind power, which has ambitious targets for PV power expansion. This case study

15 provides valuable insights into the potential benefits of diversifying the re-
16 newable energy mix on RES droughts. The performance of different RES
17 datasets are compared, and a 45-year time series of RES generation is pro-
18 duced. The results highlight the role of increased PV capacity in reducing
19 RES drought risks, offering insights for policymakers and energy planners.

20 For this study, a RES drought event is defined as occurring when the
21 average capacity factor (CF) remains below a fixed threshold for a given du-
22 ration, following the methodology used in other research [5, 6, 7, 8]. Alter-
23 native methods exist for defining RES droughts. One approach uses relative
24 CF thresholds that change over the year to account for seasonal variations in
25 renewable electricity generation [9, 10, 11, 12, 13]. Another common method
26 relies on percentile-based thresholds, where drought events are defined by
27 identifying periods of unusually low generation relative to historical pro-
28 duction levels, typically based on the lowest production percentiles [12, 14].
29 Additionally, some studies combine these definitions with metrics that in-
30 corporate the demand side of energy consumption, analysing the balance
31 between supply and demand during drought periods [9, 10, 12, 14]. In this
32 paper, the focus is exclusively on renewable electricity generation, and a fixed
33 threshold approach to define RES droughts is used, which facilitates consis-
34 tent inter-comparison between scenarios with different installed wind and PV
35 capacities.

36 RES droughts are identified using onshore wind and PV CF time series.
37 In this study, three different datasets are used, all of which are driven by
38 ERA5 data [15]. Two of the datasets are part of C3S Energy (C3S-E), an
39 energy-based operational dataset produced by the EU Copernicus Climate
40 Change Service [16, 17]. One of the C3S-E datasets provides CF time series
41 aggregated at the national scale, while the other provides the CF time series
42 at each grid point, at the ERA5 resolution of 0.25° . The third dataset was
43 generated using the Atlite model [18], which converts the ERA5 atmospheric
44 data to a generation time series using specified wind turbine and PV panel
45 models. Atlite is an open-source tool developed by PyPSA [18] and is widely
46 used for estimating wind and PV generation [7, 19, 20, 21].

47 The datasets used in this study are detailed in section 2, which describes
48 their characteristics and relevance for evaluating RES droughts. Section 3
49 outlines the RES datasets used to simulate wind and PV generation and
50 provides the methodology for defining and identifying RES drought events,
51 including the thresholds and metrics applied. In section 4, the datasets are
52 first verified against observed energy data to assess their accuracy, followed

by an analysis of RES drought occurrences for two scenarios with different ratios of installed wind to PV capacities. Finally, section 5 offers a discussion of the results in the context of energy reliability and future planning, followed by the main conclusions and recommendations for further research.

2. Data

This study uses publicly available datasets to construct and validate the datasets for estimating the CF of wind and PV energy. The primary data sources include: EirGrid and SONI, the transmission system operators (TSO) for the Republic of Ireland and Northern Ireland, respectively; the ERA5 reanalysis dataset; and the C3S-E datasets.

2.1. Wind and PV Capacity and Availability

EirGrid, the TSO for the Republic of Ireland, and SONI, the Northern Ireland TSO, provide detailed datasets on all wind and PV farms across the island of Ireland (Republic of Ireland and Northern Ireland) from 1990 to the present [22]. These datasets include information such as each farm’s installed capacity, name, and connection date. To enhance the accuracy of this data, the longitude and latitude for each farm were manually determined through online searches. For simplicity, this data will be referred to as originating from EirGrid, as all-island data was directly obtained from EirGrid, and the combined regions of the Republic of Ireland and Northern Ireland will be referred to as Ireland throughout the remainder of this document.

The spreadsheet available from the EirGrid website contains two key variables: generation and availability. Generation is the energy that a RES farm actually contributed to the grid, which may include limitations introduced by the TSO to maintain grid stability, such as constraints and curtailment. Availability represents the energy that would have been generated from a RES farm if no grid constraints had been applied, making it representative of the weather-related response. Generation and availability values are available from 2014 onward for wind power and from 2018 onward for PV power, although PV availability data only became present in the Republic of Ireland in 2023. This study focuses on availability for all analyses.

2.2. Atmospheric Variables

Atlite and C3S-E datasets are driven by the ERA5 reanalysis [15], produced by the European Centre for Medium-Range Weather Forecasts (ECMWF).

87 This global gridded dataset provides hourly atmospheric variables from 1940
88 to the present at a horizontal resolution of 0.25° . It is widely used for esti-
89 mating solar and wind energy [7, 16, 23, 24]. Table 1 lists the ERA5 variables
90 used by Atlite and C3S-Energy.

Table 1: ERA5 variables used to calculate wind and PV generation

ERA5 name	variable
100 metre zonal and meridional wind speed	u_{100}, v_{100}
2 metre temperature	$t2m$
Surface net solar radiation	ssr
Surface solar radiation downwards	$ssrd$
Top of atmosphere incident radiation	$tisr$
Total sky direct solar radiation at surface	$fdir$

91 2.3. C3S Energy

92 The EU Copernicus Climate Change Service developed the C3S-E renew-
93 able energy dataset for Europe [16], using ERA5 atmospheric variables and
94 weather-to-energy models. This dataset provides hourly CF for wind and PV
95 energy from 1979 to the present. The data are available on the same grid as
96 the ERA5 data, which has a horizontal resolution of 0.25° . The time series
97 are also available for download at two aggregated scales: regional (NUTS 2)
98 and national.

99 The C3S-E dataset estimates wind energy using wind speeds at 100 me-
100 tres (u_{100}, v_{100}) and a standard turbine model, the Vestas V136/3450, with
101 a fixed hub height of 100 meters. This choice is based on expert advice and
102 the trend in wind turbine installation. The PV generation model used by
103 C3S-E uses two ERA5 variables: surface solar radiation downwards ($ssrd$)
104 and air temperature ($t2m$). PV generation is calculated multiple times, us-
105 ing the same model with different azimuth and tilt angles. The results are
106 aggregated based on a statistical distribution of the module angles based on
107 the geographical location [25].

108 3. Methods

109 This study uses three datasets to analyse RES droughts across the island
110 of Ireland. Data downloaded from C3S-E were used to obtain two datasets:
111 one based on national-level data (C3S-E N), and another on grid-level data
112 (C3S-E G). The third dataset was computed using the Atlite model (Atlite).

113 3.1. C3S-Energy National

114 For national-level analyses, the aggregated CF time series provided by
115 C3S-E were used at two levels: Republic of Ireland (NUTS0: IE) and North-
116 ern Ireland (NUTS2: UKN0). These are based on the assumption by C3S-E
117 that RES generation occurs at every ERA5 grid point in Ireland. We com-
118 puted a weighted average of these, based on the installed capacity of each
119 one, to represent the total CF for Ireland.

120 3.2. C3S-E Gridded

121 The gridded dataset from C3S-E was used to create CF datasets which
122 account for the location of RES farms in Ireland. A list of the RES farms in
123 Ireland was compiled, including each farm’s latitude, longitude and installed
124 capacity. Using these coordinates, the nearest grid point on the C3S-E grid
125 was identified for each farm. The CF values from the C3S-E dataset corre-
126 sponding to these grid points were retrieved. A weighted average of the CF
127 values was calculated, with the installed capacity of each farm serving as the
128 weight, to construct the CF time series for Ireland. This process resulted in
129 a time series of RES generation for each energy source (wind and PV) for
130 Ireland, which takes the location of the RES farms into account.

131 3.3. Atlite

132 Atlite transforms weather data into energy data using the gridded ERA5
133 data and the locations of existing RES farms, as described in C3S-E G.
134 ERA5 data for wind speed at 100 metres (u_{100} , v_{100}) are used to calculate
135 wind generation, while the ERA5 radiation variables (ssr , $ssrd$, $tisr$, and
136 $fdir$) and air temperature ($t2m$) are used to calculate PV generation. A
137 key distinction between C3S-E and Atlite lies in their representation of wind
138 turbines and PV panels. This study identifies the most appropriate wind
139 turbine power curve to use from the 121 power curves made available by
140 Renewables.ninja [26]. The selection of a specific wind turbine and PV panel
141 characteristics is further discussed and explained in section 4.1.

142 3.4. Energy Scenarios

143 In addition to analysing wind and PV generation separately, a combined
144 CF was computed for each dataset by averaging wind and PV generation,
145 weighted by their installed capacities at the end of 2023 (5.9 GW for wind
146 power and 0.6 GW for PV power). This configuration is referred to as the

147 91W-9PV scenario, reflecting the distribution of 91% wind and 9% PV ca-
 148 pacity. Given that PV capacity in Ireland is low in 2023, and to explore how
 149 a more balanced distribution of wind and PV capacities might impact RES
 150 droughts, this study also considered a second scenario, referred to as 57W-
 151 43PV, where the installed PV capacity is assumed to increase to 8.6 GW,
 152 while wind capacity rises to 11.45 GW. These values are based on targets
 153 outlined in the roadmap published by the 2024 Climate Action Plan [27].
 154 This study does not include offshore wind in the analysis. Recent reports
 155 suggest that even by 2030, Ireland is unlikely to have any significant new off-
 156 shore wind farms, with projected offshore capacity expected to remain near
 157 zero using realistic scenarios [28].

158 New time series were generated for both the Atlite and C3S-E G PV
 159 datasets, incorporating a revised distribution of installed capacity across Ire-
 160 land as specified in the roadmap. For wind power, the CF time series remains
 161 unchanged, as significant shifts in the location of wind farms are not expected.
 162 In total, twelve CF time series were analysed in this study, six for individual
 163 wind and PV CF (three models for each source) in the 91W-9PV scenario,
 164 and an additional six time series that include the combined CF for 91W-9PV
 165 and 57W-43PV scenarios across the different models.

166 It is important to note that the specific capacity values used in this study
 167 are illustrative and are not intended to reflect precise future realities. Instead,
 168 they serve to explore the impact of transitioning from a wind-dominated sys-
 169 tem (91W-9PV) to a more evenly distributed system (57W-43PV). This ap-
 170 proach allows for a comparative analysis between the two scenarios, assessing
 171 how the balance of RES capacity affects the occurrence of RES droughts.

172 3.5. RES Drought Definition

173 In this study, a RES drought event was defined as occurring when the
 174 24-hour moving average of CF remains below a fixed threshold of 0.1 for
 175 a period of longer than 24 hours. The choice of this threshold is somewhat
 176 arbitrary, but aligns with similar studies on low renewable energy production
 177 [5, 6, 8]. By using a 24-hour moving average, fewer but longer-lasting events
 178 were captured compared to using the raw CF time series, which can be more
 179 sensitive to short-term fluctuations. A fixed threshold approach was chosen
 180 in this study to enable consistent inter-comparison between datasets.

181 The moving average approach smooths out short-term fluctuations, so
 182 that brief periods above the threshold do not interrupt an otherwise con-
 183 tinuous low-CF period (Fig. 1). This means that a single hour above the

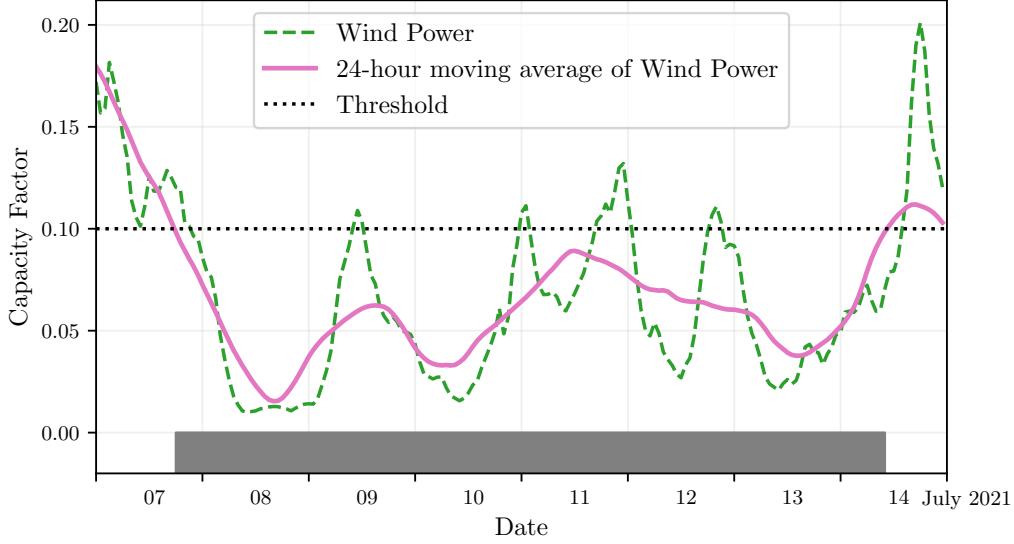


Figure 1: Wind time series of CF (green) and its 24-hour moving average (pink) from the 7th to the 15th of July 2021. The black dashed line indicates the CF threshold. The grey bar shows the period identified as a wind drought under our definition

184 threshold does not "break" a drought event if it is surrounded by prolonged
 185 low-generation hours. As a result, fewer but longer-lasting drought events
 186 are identified, which may better reflect real-world conditions where energy
 187 supply constraints persist over extended periods.

188 4. Results

189 4.1. Verification

190 The accuracy of the datasets used in this study was verified, before con-
 191 tinuing to the analysis of RES droughts. For the verification process, time-
 192 varying values of installed capacity were used to account for changes in RES
 193 development over the verification period. This step allowed us to assess how
 194 well the datasets represent the production of renewable energy by comparing
 195 them against observed data.

196 4.1.1. Wind Energy

197 The C3S-E datasets use the Vestas V136/3450 wind turbine power curve,
 198 (Fig. 2a). The Atlite model allows the user to specify the power curve.

199 We considered the 121 power curves available for download from Renew-
 200 ables.ninja [26]. For each power curve, Renewables.ninja also provides four
 201 associated smoothed power curves. The smoothing is done using a Gaussian
 202 filter with different standard deviations that depend on the wind speed. A
 203 separate wind CF time series for Ireland was generated for each of the wind
 204 turbine power curves and smoothing levels.

205 The performance of each CF time series is then assessed based on four skill
 206 scores: correlation coefficient (CC), root mean square error (RMSE), mean
 207 bias error (MBE), and the percentage of overlap. The percentage of overlap
 208 quantifies the similarity between the observed and modelled distributions. It
 209 is a positively oriented skill score, where 100% shows full agreement between
 210 the two distributions, and 0% indicates no overlap. The histograms of hourly
 211 CF values for the most recent decade (2014-2023) are used to calculate this
 212 skill score.

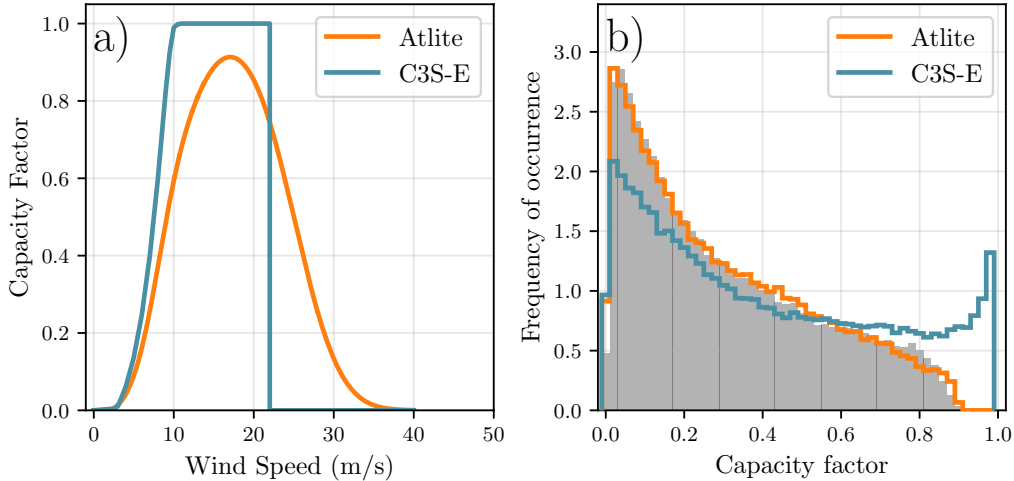


Figure 2: a) Power curves of the Enercon E112.4500 with a $0.3w$ smoothing filter used by Atlite (orange) and the Vestas V136/3450 used by C3S-E (blue) b) Histograms of wind CF for Ireland from Atlite (orange), C3S-E (blue) and Observed (shaded)

213 Based on these metrics, the most representative power curve for Ireland
 214 is the Enercon E112.4500 power curve with the $0.3w$ smoothing filter. The
 215 smoothing of the wind turbine power curve represents losses associated with
 216 each turbine, as well as losses such as wake effects between turbines, which
 217 are important when modelling wind energy on larger spatial scales. The his-
 218 togram in Fig. 2b shows that the C3S-E power curve tends to underestimate

low CF values and overestimate higher ones, whereas the smoothed Atlite power curve more closely follows the observed wind availability data. This is further supported by the percentage of overlap which is higher for Atlite (97.2%) than for C3S-E (83.2%), indicating better agreement with observed data.

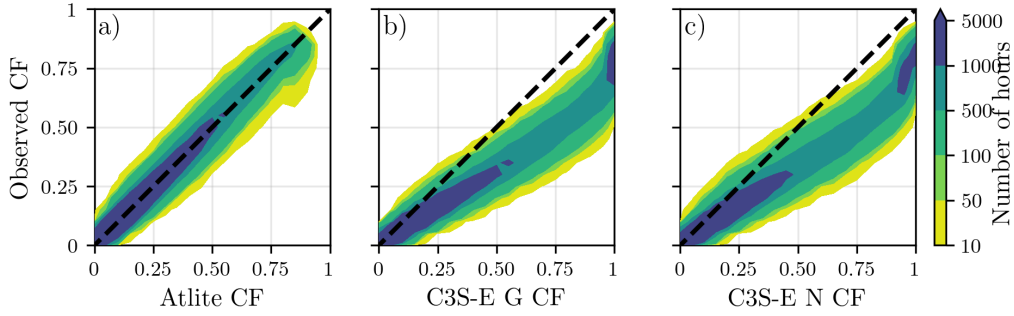


Figure 3: Wind CF density plot of the observed CF (vertical axes) and modelled (horizontal axes) CF data for the a) Atlite, b) C3S-E G and c) C3S-E N models

The effect of the difference between the power curves is also visible in Fig. 3, which shows a density plot of wind CF values. The two C3S-E datasets are shown to overestimate the observed CF, whereas the Atlite model is in good agreement with the observed data. The skill scores presented in Table 2 show that Atlite performs better than the C3S-E datasets for all of the skill scores.

	Atlite	C3S-E G	C3S-E N
CC	0.981	0.972	0.970
RMSE	0.045	0.177	0.162
MBE	-0.003	0.137	0.121

Table 2: Skill scores for wind power for the three datasets compared to observed data

Fig. 4 shows the average annual number of wind drought events during the 2014 to 2023 validation period. The figure reveals that Atlite presents the best overall agreement with the observed frequency and duration of wind drought events. This pattern is particularly evident for shorter-duration events, which are the most frequent.

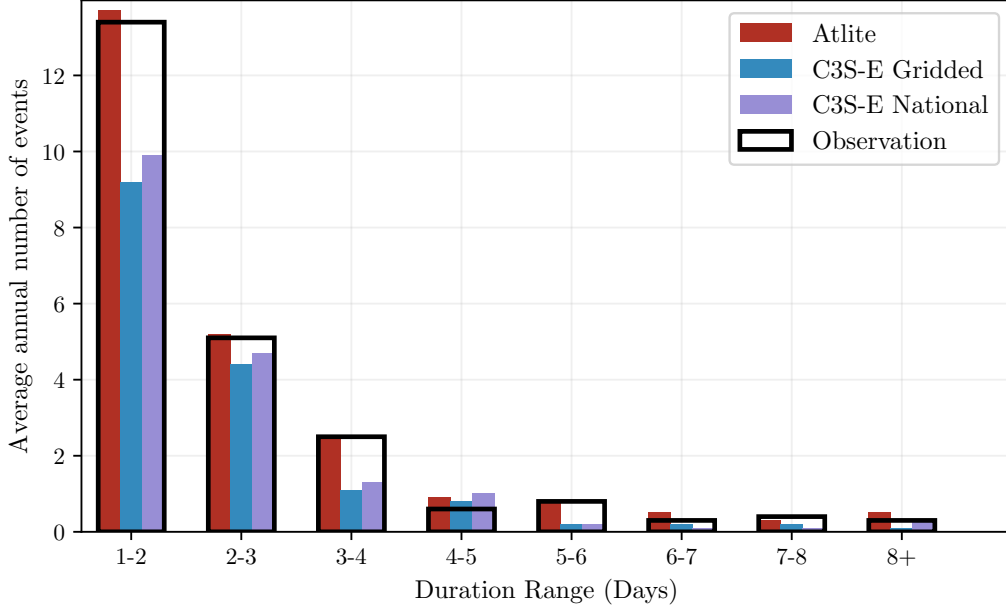


Figure 4: Average annual number of wind drought events for Atlite (red), C3S-E G (blue), C3S-E N (purple), and the observed data (black outline). The wind droughts are identified from 2014 to 2023, considering the actual capacity of the system at any given time

235 4.1.2. PV Energy

236 The Atlite model allows the user to select certain PV panel characteristics.
 237 In this study, the three PV panel types available in the Atlite model were
 238 considered (CSi, CdTe, Kaneka). Following the same methodology as in the
 239 previous section, the three available models were compared using four skill
 240 scores (CC, RMSE, MBE, and the percentage of overlap). Based on the best-
 241 performing metrics, the Beyer PV panel model was selected [29], using the
 242 Kaneka Hybrid panel option. For all PV farm locations, the azimuth angle
 243 is fixed at 180° (due south), and the optimal tilt angle option is applied.

244 The PV installed capacity available on the spreadsheets from EirGrid
 245 represents the Maximum Export Capacity (MEC) and does not accurately
 246 reflect the installed PV capacity. To enable actual PV generation potential
 247 to be modelled correctly, installed capacities were set at 1.4 times the MEC
 248 values. This scaling factor was estimated by analysing proprietary data from
 249 individual PV farms provided by EirGrid, which showed that, on average,
 250 assuming that the installed capacities of farms exceed their MEC values by

251 40% yields the best agreement with the observed availability.

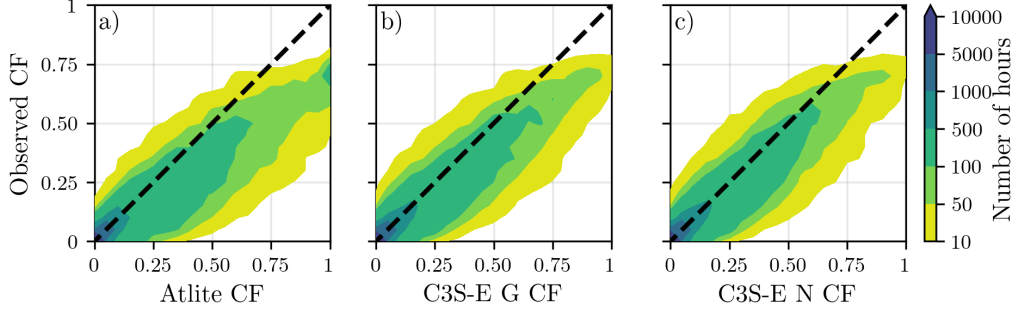


Figure 5: PV CF density plot of the observed (vertical axes) and modelled (horizontal axes) CF series for the a) Atlite, b) C3S-E G and c) C3S-E N datasets

252 Figure 5 shows that the three datasets have a similar tendency to overesti-
 253 mate the CF compared to the observed values, especially for high CF values.
 254 The skill scores presented in Table 3 indicate that C3S-E G performs best
 255 overall, with the lowest RMSE and a high correlation coefficient, suggesting
 256 a closer match to observed data. All models show a slight positive bias, with
 257 Atlite exhibiting a slightly lower correlation and higher RMSE.

	Atlite	C3S-E G	C3S-E N
CC	0.921	0.931	0.931
RMSE	0.119	0.090	0.113
MBE	0.046	0.027	0.021

Table 3: Skill scores for PV CF for the three datasets compared to observed data

258 Fig. 6 shows the number of PV drought events during the 2023 validation
 259 period across different duration ranges. The figure reveals partial agreement
 260 between the three datasets and the observed data, with consistent results
 261 noticed for duration ranges of 1-2, 3-4, 7-8, and 8+ days. However, dis-
 262 crepancies appear in the other ranges, where the models diverge from the
 263 observed data. The main challenge in validating PV data stems from the
 264 recent installation of a large share of Ireland’s PV capacity, with over 65%
 265 of the total PV capacity installed in 2023. This results in uncertainties in PV
 266 generation data and the actual generating capacity in the first few months
 267 after each farm is connected.

268 As the goal of this analysis is to assess the combination of wind and PV
 269 generation, the complementary nature of these energy sources mitigates the
 270 limitations in PV-only results.

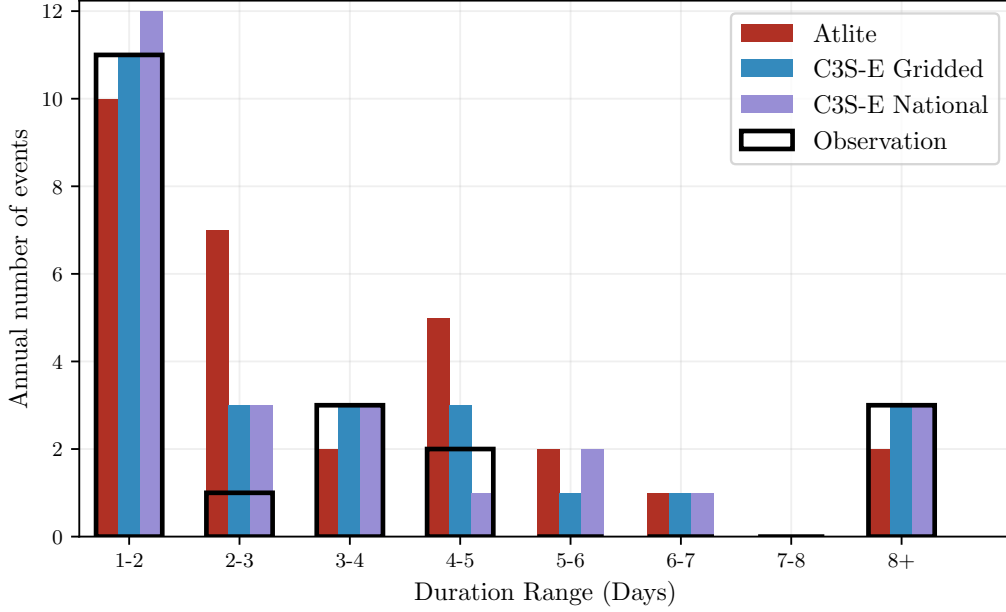


Figure 6: Number of PV drought events for Atlite (red), C3S-E G (blue), and C3S-E N (purple) and the observed data (black outline). The PV droughts are identified for 2023, considering the actual capacity of the system at any given time

271 4.2. Analysis

272 In this section, RES drought events are evaluated under two different
 273 scenarios with fixed installed capacities: the 91W-9PV scenario, with 5.9 GW
 274 of wind capacity and 0.6 GW of PV capacity; and the 57W-43PV scenario,
 275 where wind capacity comprises 11.45 GW and PV capacity increases to 8.6
 276 GW. Both scenarios were driven by 45 years of ERA5 data. Using the RES
 277 drought identification process described in Section 3.5, wind and PV droughts
 278 are first analysed separately before presenting the results for combined (wind
 279 + PV) RES droughts under both scenarios.

280 4.2.1. Annual Number of RES Droughts

281 The first part of the analysis examines the annual number of RES drought
 282 events across the three datasets. When only wind energy is considered

(Fig. 7a), the number of events decreases as the duration range increases, with very few events lasting more than seven days. In the case of only PV energy (Fig. 7b), the number of events also declines as the duration range extends from one to eight days, followed by a slight increase for longer durations. This increase occurs because Ireland, being located above the 50° parallel, experiences reduced sunlight during the winter months. From November to March, PV output often remains consistently low, leading to extended periods where generation stays below the CF threshold.

When comparing wind and PV results (Fig. 7a & b), the median, first, and third quartiles for PV are consistently higher than or equal to those for wind, across all duration ranges and datasets. This is due to the typically lower CF of PV power compared to wind power, especially in a region such as Ireland where solar potential is limited. PV generation is also zero at night and constrained by the daily solar cycle, leading to a naturally higher frequency of drought events in PV compared to wind.

Fig. 7c & d show the combination of wind and PV under the two capacity scenarios. In the 91W-9PV scenario (Fig. 7c), the identified RES droughts closely match those for wind alone, which is expected due to the dominance of installed wind capacity. In contrast, the 57W-43PV scenario (Fig. 7d) shows a clear reduction in the number of drought events across all datasets and durations, with a decrease of the total number of events of 56% for Atlite, 52% for C3S-E G, and 50% for C3S-E N. This reduction is attributed to the anti-correlation between wind and PV generation.

The median, first, and third quartiles for the Atlite dataset are consistently greater than or equal to those of the other two datasets, regardless of the duration range or type of renewable energy considered. This difference arises from the wind turbine power curve model used in the C3S-E datasets, which tends to overestimate the wind CF (Fig. 3). As a result, the overall number of RES droughts is underestimated in the C3S-E datasets compared to Atlite.

4.2.2. Return Periods of RES Drought Duration

The RES drought events identified over the 45-year period were used to calculate the return periods for different RES drought durations. A return period is the estimated average time interval between events of a specified duration or intensity (not to be confused with the frequency of their occurrence within a fixed time frame). Fig. 8 illustrates the return periods for varying RES drought durations, highlighting how often different drought lengths are

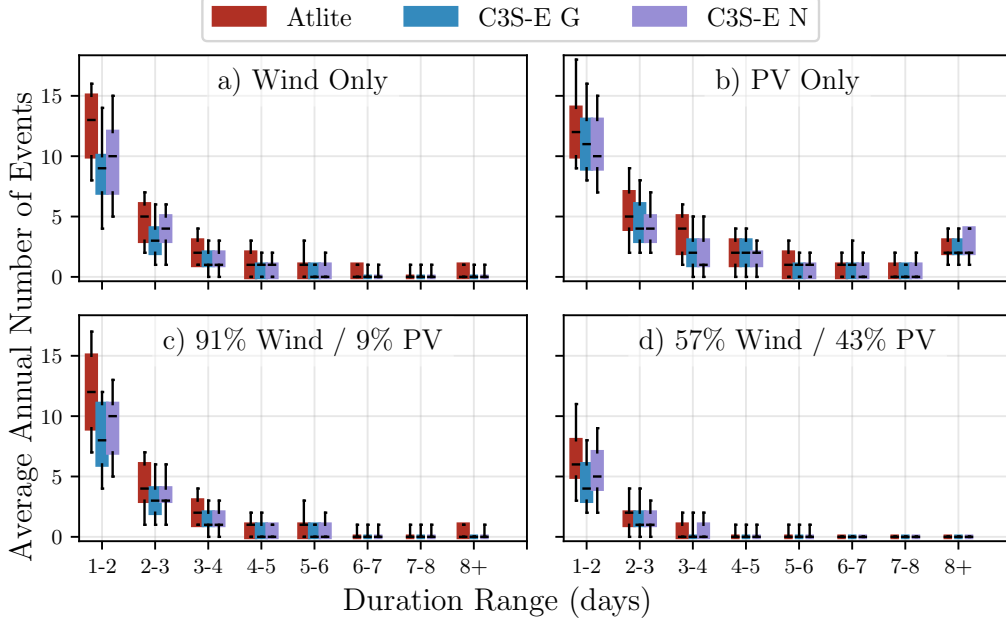


Figure 7: Average annual number of RES droughts (from 1979 to 2023) for a) Wind, b) PV, c) 91W-9PV and d) 57W-43PV for Atlite (red), C3S-E G (blue), and C3S-E N (purple). The x-axis represents duration ranges in days (lower bound included), while the y-axis indicates the annual number of events. The boxes display the first and third quartiles and the median is marked by a black line. The whiskers indicate the 5th and 95th percentiles

likely to occur across the datasets. This analysis provides insight into the frequency and likelihood of prolonged low-generation periods, which is crucial for evaluating the potential impact of RES droughts on energy reliability and security of supply.

The duration of wind droughts (Fig. 8a) increases in a log-linear fashion across the three datasets. The log-linear trend indicates a predictable relationship between drought duration and occurrence, with longer wind droughts becoming exponentially less likely as duration increases.

In the case of PV droughts (Fig. 8b), Atlite behaves differently than the two C3S-E datasets. The Atlite results show a generally log-linear increase. For C3S-E G and C3S-E N, the duration of PV droughts increases in a log-linear pattern for events lasting less than 16 days. Beyond this duration, there is a sharp rise in drought duration for events up to a one-year return period. This sudden increase again reflects the impact of extended periods

334 of low PV generation during winter in Ireland.

335 The difference between Atlite and the C3S-E results arises from differ-
336 ences in the datasets near the threshold of 0.1 CF. Atlite remains slightly
337 above the threshold more frequently during these conditions, leading to
338 shorter, more fragmented drought events. In contrast, C3S-E G and C3S-E
339 N tend to fall below the threshold in similar conditions, resulting in longer
340 continuous drought periods, especially during winter.

341 For the 91W-9PV scenario (Fig. 8c), the return periods mirror those of
342 Fig. 8a, due to the low levels of installed PV capacity. In the 57W-43PV
343 scenario (Fig. 8d), the return periods for RES droughts increase across all
344 durations. For example, the return period for a five-day drought event (shown
345 by the vertical dashed lines in Fig. 8) extends from roughly six months for
346 the 91W-9PV scenario, to four years for the 57W-43PV scenario in the Atlite
347 dataset, and from about fifteen months to around five years in the two C3S-E
348 datasets.

349 Across Fig. 8a, c, and, d, the return periods in the Atlite dataset are
350 consistently higher than those in the two C3S-E datasets. For instance, in
351 the 91W-9PV scenario (Fig. 8c), an event with a one-year return period
352 lasts six days in the Atlite dataset, compared to only five days in the C3S-E
353 datasets. This difference underscores the importance of model selection when
354 quantifying RES droughts, as each model’s assumptions and parametrisations
355 significantly influence drought duration estimates. Additionally, in all four
356 graphs, the similarity between results from the two C3S-E datasets suggests
357 that assumptions in the Atlite model—such as wind turbine power curve
358 selection and PV panel specifications—have a greater impact on RES drought
359 duration estimates than the precise geographic distribution of RES farms
360 when studying the return periods of RES droughts.

361 4.2.3. Seasonal Distribution of RES Droughts

362 The seasonality of RES droughts was analysed by comparing the percent-
363 age of hours in each month classified as part of a RES drought.

364 For wind-dominated scenarios (Fig. 9a & c), the percentage of hours that
365 are part of a drought is higher in summer than in winter. In the Atlite
366 dataset, for instance, an average of 24% of hours in summer (June-July-
367 August) are identified as wind droughts, compared to only 4% in winter
368 (December-January-February). This seasonal variation is less prominent for
369 the two C3S-E datasets compared to the Atlite one. This difference can be
370 linked to the shape of the two power curves (Fig. 2). CFs near or under the

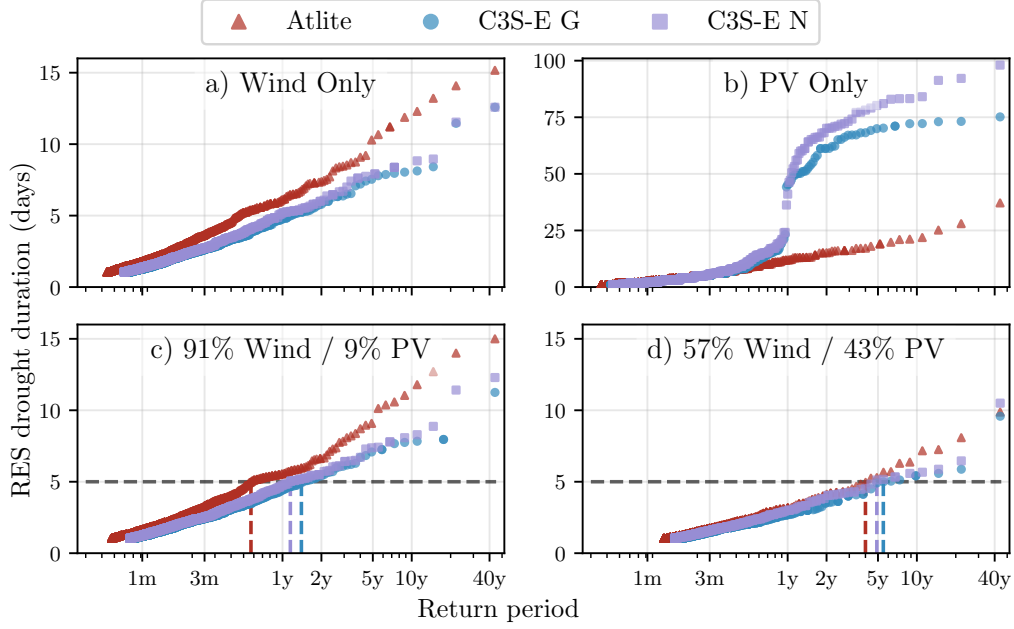


Figure 8: Return periods of the duration of RES droughts (from 1979 to 2023) for a) Wind, b) PV, c) 91W-9PV and d) 57W-43PV for Atlite (red triangle), C3S-E G (blue circle), and C3S-E N (purple square). The x-axis represents the return period time in a log-scale and the y-axis indicates the duration of RES drought associated with it. The horizontal dashed line marks the 5-day return period, with coloured vertical dashed marking its return period for each dataset

0.1 threshold occur at higher wind speeds for the Atlite power curve than for the C3S-E one. In contrast, the results for PV droughts (Fig. 9b) show a higher percentage in winter, with PV droughts occurring over 60% of the time regardless of the dataset. The Atlite results show a higher percentage of PV drought hours for wind, and a slightly lower percentage for PV, compared to the two C3S-E datasets.

The 91W-9PV scenario (Fig. 9c) shows patterns comparable to the ones for wind droughts (Fig. 9a). However, in the 91W/9PV scenario, the number of hours classified as RES droughts in summer decreases slightly compared to the wind-only scenario. This reduction can be explained by the contribution of PV generation during the summer months in the 91W-9PV scenario, even though it constitutes only 11% of total capacity. Since the number of RES drought hours for PV in summer is near zero, this small contribution has a

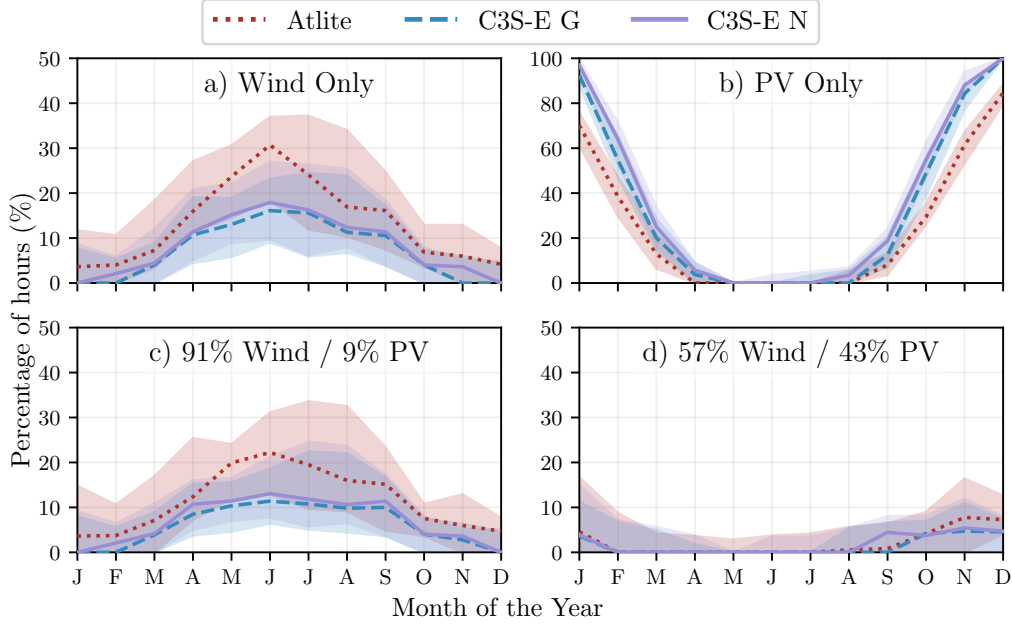


Figure 9: Percentage of hours in a month which are part of a RES drought (from 1979 to 2023) for a) Wind, b) PV, c) 91W-9PV and d) 57W-43PV for Atlite (red dotted), C3S-E G (blue dashed), and C3S-E N (purple solid). The x-axis represents the month of the year, and the y-axis indicates the percentage of hours. Lines correspond to the median values and the area between the first and third quartiles is shaded. Note the different y-axis scale for b).

noticeable impact on reducing overall drought hours. In the 57W-43PV scenario (Fig. 9d), all three datasets show a reduction in monthly RES drought frequency. Annual reductions in median RES drought frequency are observed across the datasets, dropping from 14% to 5% for Atlite, from 8% to 3% for C3S-E G, and from 9% to 4% for C3S-E N. The balanced mix of wind and PV power in this scenario reduces the seasonal signal overall and significantly decreases the percentage of RES drought hours in the summer.

5. Discussion and Conclusions

This study has investigated the ability of three RES models to represent RES droughts: Atlite, C3S-E G, and C3S-E N. One of the most evident differences is how each dataset incorporates the specific locations of RES farms. Both Atlite and C3S-E G consider the locations of wind and PV

396 farms, which one would expect to result in a more accurate representation
397 of RES generation. While this approach slightly improves PV models, our
398 analysis indicates that for wind energy, the Atlite dataset performs better
399 overall, especially in its close alignment with observed data for wind gener-
400 ation estimates. This finding suggests that, although the inclusion of RES
401 farm locations is beneficial, the accuracy of the RES model is more strongly
402 influenced by underlying model assumptions, such as selecting an appropriate
403 wind power curve.

404 Atlite shows the best alignment with observed data for wind generation.
405 Differences between the models are smaller for PV, with C3S-G performing
406 marginally better than the other two. The results show that the two C3S-E
407 datasets (C3S-E G and C3S-E N) consistently yield similar outcomes, in-
408 dicating that their methodological differences have minimal impact in this
409 case. This distinction is also evident in the analysis, where Atlite reports
410 higher return periods and a greater number of RES droughts, especially in
411 scenarios with a balanced share of RES. Again, the results from RES drought
412 modelling rely more on the precision of the wind power curve and PV panel
413 models than on the specific locations of RES farms. Atlite’s superior perfor-
414 mance highlights the importance of selecting validated models for assessing
415 RES drought risks. This careful model selection can better quantify risks,
416 support effective planning, and avoid the potential underestimation of ca-
417 pacity needs, which is essential for ensuring energy security.

418 Looking at the 57W-43PV scenario, the analysis showed a significant im-
419 provement in the management of RES droughts due to the complementary
420 nature of wind and PV generation. Wind and PV together perform better
421 in terms of reducing drought frequency and duration than either would in-
422 dividually, largely because of the seasonal anti-correlation between the two
423 energy sources. This diversification reduces the seasonal impact on RES
424 droughts, as PV generation peaks in the summer and wind generation is
425 more consistent in winter. Ireland currently has a highly wind-dependent
426 energy system, but with ambitious targets for PV installations in the coming
427 years, the energy mix is expected to approach a balance between wind and
428 PV capacity. While this balanced approach offers a more stable and secure
429 energy supply by mitigating RES drought risks, it is important to note that
430 having similar wind and PV capacities may not optimise other aspects, such
431 as annual energy production or meeting nighttime loads. For policymakers,
432 these findings underscore the importance of meeting these capacity targets
433 to enhance energy security through diversification. Additionally, the choice

434 of model for RES drought assessment becomes increasingly critical as more
435 renewable capacity is integrated into the system.

436 Future work is planned to extend the current analysis. First, climate
437 projection data will be integrated with different energy scenarios, incorpo-
438 rating the addition of offshore wind, to better understand how climate change
439 might affect RES droughts. Second, expanding the geographic domain of the
440 study to include the rest of Europe would provide a more comprehensive un-
441 derstanding of RES droughts in an interconnected energy grid. This would
442 require extensive verification across other European countries, making it a
443 more complex but highly relevant challenge.

444 Data Availability

445 The ERA5 data can be obtained from the Climate Data Store (<https://doi.org/10.24381/cds.adbb2d47>). The C3S-E dataset is also available
446 from the Climate Data Store (<https://doi.org/10.24381/cds.4bd77450>).
447 Information on wind and PV farms in Ireland can be obtained from the
448 EirGrid website ([https://www.eirgrid.ie/grid/system-and-renewable](https://www.eirgrid.ie/grid/system-and-renewable-data-reports)
449 [-data-reports](https://www.eirgrid.ie/grid/system-and-renewable-data-reports)). The Atlite model used in this study is open-source and can
450 be found on GitHub (<https://github.com/pypsa/atlite>). The data and
451 code required to reproduce the analysis in this article will be made available
452 upon acceptance of the manuscript in a public GitHub repository.

454 Acknowledgments

455 The research conducted in this publication was funded by Science Foun-
456 dation Ireland and co-funding partners under grant number 21/SPP/3756
457 through the NexSys Strategic Partnership Programme.

458 References

- 459 [1] EuroStat, Renewable Energy Statistics, 2023. URL: [https://ec.europa.eu/eurostat/statistics-explained/index.php?title=Renewable](https://ec.europa.eu/eurostat/statistics-explained/index.php?title=Renewable_energy_statistics)
460 [energy_statistics](https://ec.europa.eu/eurostat/statistics-explained/index.php?title=Renewable_energy_statistics), Accessed: 2024-11-06.
- 462 [2] H. C. Bloomfield, D. J. Brayshaw, L. C. Shaffrey, P. J. Coker, H. E.
463 Thornton, Quantifying the increasing sensitivity of power systems to
464 climate variability, *Environmental Research Letters* 11 (2016) 124025.
465 doi:10.1088/1748-9326/11/12/124025.

- 466 [3] H. C. Bloomfield, D. J. Brayshaw, A. Troccoli, C. M. Goodess, M. De Fe-
467 lice, L. Dubus, P. E. Bett, Y.-M. Saint-Drenan, Quantifying the
468 sensitivity of european power systems to energy scenarios and cli-
469 mate change projections, *Renewable Energy* 164 (2021) 1062–1075.
470 doi:10.1016/j.renene.2020.09.125.
- 471 [4] K. van der Wiel, L. P. Stoop, B. R. H. Van Zuijlen, R. Blackport, M. A.
472 Van den Broek, F. M. Selten, Meteorological conditions leading to ex-
473 treme low variable renewable energy production and extreme high en-
474 ergy shortfall, *Renewable and Sustainable Energy Reviews* 111 (2019)
475 261–275. doi:10.1016/j.rser.2019.04.065.
- 476 [5] F. Kaspar, M. Borsche, U. Pfeifroth, J. Trentmann, J. Drücke, P. Becker,
477 A climatological assessment of balancing effects and shortfall risks of
478 photovoltaics and wind energy in germany and europe, *Advances in*
479 *Science and Research* 16 (2019) 119–128. doi:10.5194/asr-16-119-2
480 019.
- 481 [6] M. Ohba, Y. Kanno, D. Nohara, Climatology of dark doldrums in japan,
482 *Renewable and Sustainable Energy Reviews* 155 (2022) 111927. doi:10
483 .1016/j.rser.2021.111927.
- 484 [7] F. Mockert, C. M. Grams, T. Brown, F. Neumann, Meteorological
485 conditions during periods of low wind speed and insolation in Germany:
486 The role of weather regimes, *Meteorological Applications* 30 (2023)
487 e2141. doi:10.1002/met.2141.
- 488 [8] M. J. Mayer, B. Biró, B. Szücs, A. Aszódi, Probabilistic modeling of
489 future electricity systems with high renewable energy penetration using
490 machine learning, *Applied Energy* 336 (2023) 120801. doi:10.1016/j.
491 apenergy.2023.120801.
- 492 [9] D. Raynaud, B. Hingray, B. François, J. Creutin, Energy droughts from
493 variable renewable energy sources in European climates, *Renewable*
494 *Energy* 125 (2018) 578–589. doi:https://doi.org/10.1016/j.renene
495 .2018.02.130.
- 496 [10] K. Z. Rinaldi, J. A. Dowling, T. H. Ruggles, K. Caldeira, N. S. Lewis,
497 Wind and Solar Resource Droughts in California Highlight the Benefits
498 of Long-Term Storage and Integration with the Western Interconnect,

- 499 Environmental Science and Technology 55 (2021) 6214–6226. doi:10.1
500 021/acs.est.0c07848.
- 501 [11] A. Gangopadhyay, A. K. Seshadri, N. J. Sparks, R. Toumi, The role
502 of wind-solar hybrid plants in mitigating renewable energy-droughts,
503 Renewable Energy 194 (2022) 926–937. doi:10.1016/j.renene.2022.
504 05.122.
- 505 [12] S. Allen, N. Otero, Standardised indices to monitor energy droughts,
506 Renewable Energy 217 (2023) 119206. doi:10.1016/j.renene.2023.11
507 9206.
- 508 [13] J. Kapica, J. Jurasz, F. A. Canales, H. Bloomfield, M. Guezgouz,
509 M. De Felice, Z. Kobus, The potential impact of climate change on
510 european renewable energy droughts, Renewable and Sustainable En-
511 ergy Reviews 189 (2024) 114011. doi:10.1016/j.rser.2023.114011.
- 512 [14] C. Bracken, N. Voisin, C. D. Burleyson, A. M. Campbell, Z. J. Hou,
513 D. Broman, Standardized benchmark of historical compound wind and
514 solar energy droughts across the Continental United States, Renewable
515 Energy 220 (2024) 119550. doi:https://doi.org/10.1016/j.renene
516 .2023.119550.
- 517 [15] H. Hersbach, B. Bell, P. Berrisford, S. Hirahara, A. Horányi, J. Muñoz-
518 Sabater, J. Nicolas, C. Peubey, R. Radu, D. Schepers, et al., The ERA5
519 global reanalysis, Quarterly Journal of the Royal Meteorological Society
520 146 (2020) 1999–2049. doi:10.1002/qj.3803.
- 521 [16] L. Dubus, Y. Saint-Drenan, A. Troccoli, M. De Felice, Y. Moreau, L. Ho-
522 Tran, C. Goodess, R. Amaro E Silva, L. Sanger, C3S Energy: A climate
523 service for the provision of power supply and demand indicators for Eu-
524 rope based on the ERA5 reanalysis and ENTSO-E data, Meteorological
525 Applications 30 (2023) e2145. doi:10.1002/met.2145.
- 526 [17] Copernicus Climate Change Service (C3S), Climate and energy indi-
527 cators for Europe from 1979 to present derived from reanalysis., 2020.
528 doi:10.24381/cds.4bd77450, accessed on 28-11-2024.
- 529 [18] F. Hofmann, J. Hampp, F. Neumann, T. Brown, J. Hörsch, Atlite: a
530 lightweight Python package for calculating renewable power potentials

- 531 and time series, *Journal of Open Source Software* 6 (2021) 3294. doi:10
532 .21105/joss.03294.
- 533 [19] J. Li, Z. Zhao, D. Xu, P. Li, Y. Liu, M. A. Mahmud, D. Chen, The
534 potential assessment of pump hydro energy storage to reduce renewable
535 curtailment and CO2 emissions in Northwest China, *Renewable Energy*
536 212 (2023) 82–96. doi:10.1016/j.renene.2023.04.132.
- 537 [20] M. Parzen, H. Abdel-Khalek, E. Fedotova, M. Mahmood, M. M. Frysztacki,
538 J. Hampp, L. Franken, L. Schumm, F. Neumann, D. Poli,
539 et al., Pypsa-earth. a new global open energy system optimization
540 model demonstrated in africa, *Applied Energy* 341 (2023) 121096.
541 doi:10.1016/j.apenergy.2023.121096.
- 542 [21] K. Ali Khan Niazi, M. Victoria, Comparative analysis of photovoltaic
543 configurations for agrivoltaic systems in europe, *Progress in Photo-*
544 *voltatics: Research and Applications* 31 (2023) 1101–1113. doi:10.1002/
545 pip.3727.
- 546 [22] EirGrid & SONI, System and Renewable Data Reports, 2023. URL:
547 [https://www.eirgrid.ie/grid/system-and-renewable-data-rep](https://www.eirgrid.ie/grid/system-and-renewable-data-reports)
548 [orts](https://www.eirgrid.ie/grid/system-and-renewable-data-reports), Accessed: 2024-11-06.
- 549 [23] P. T. Brown, D. J. Farnham, K. Caldeira, Meteorology and climatology
550 of historical weekly wind and solar power resource droughts over western
551 North America in ERA5, *SN Applied Sciences* 3 (2021) 814. doi:10.1
552 007/s42452-021-04794-z.
- 553 [24] N. Otero, O. Martius, S. Allen, H. Bloomfield, B. Schaeffli, Character-
554 izing renewable energy compound events across Europe using a logistic
555 regression-based approach, *Meteorological Applications* 29 (2022) e2089.
556 doi:10.1002/met.2089, 13.
- 557 [25] Y.-M. Saint-Drenan, L. Wald, T. Ranchin, L. Dubus, A. Troccoli, An
558 approach for the estimation of the aggregated photovoltaic power gener-
559 ated in several European countries from meteorological data, *Advances*
560 *in Science and Research* 15 (2018) 51–62. doi:10.5194/asr-15-51-201
561 8.

- 562 [26] I. Staffell, S. Pfenninger, Using bias-corrected reanalysis to simulate
563 current and future wind power output, *Energy* 114 (2016) 1224–1239.
564 doi:10.1016/j.energy.2016.08.068.
- 565 [27] Government of Ireland, Climate Action Plan 2024, Technical Report 3,
566 Department of the Environment, Climate and Communications, 2023.
567 URL: [https://www.gov.ie/pdf/?file=https://assets.gov.ie/](https://www.gov.ie/pdf/?file=https://assets.gov.ie/284675/70922dc5-1480-4c2e-830e-295afd0b5356.pdf)
568 [284675/70922dc5-1480-4c2e-830e-295afd0b5356.pdf](https://www.gov.ie/pdf/?file=https://assets.gov.ie/284675/70922dc5-1480-4c2e-830e-295afd0b5356.pdf), Accessed:
569 2024-11-06.
- 570 [28] Sustainable Energy Authority Ireland, National Energy Projections
571 2024, Technical Report, Sustainability Energy Authority of Ireland,
572 2024. URL: [https://www.seai.ie/news-and-events/news/energ](https://www.seai.ie/news-and-events/news/energy-projections-report)
573 [y-projections-report](https://www.seai.ie/news-and-events/news/energy-projections-report), Accessed: 2024-11-06.
- 574 [29] H. G. Beyer, G. Heilscher, S. Bofinger, A robust model for the mpp
575 performance of different types of pv-modules applied for the performance
576 check of grid connected systems, *Eurosun* (2004) 8.